Journal of
Ceramic Science
and Technology

J. Ceram. Sci. Tech., **04** [03] 163-168 (2013)
DOI: 10.4416/JCST2013-00009
available online at: http://www.ceramic-science.com

In Vitro Characterization of Carbon-Nanotube-Reinforced Hydroxyapatite Composite Coating on 316L Stainless Steel

S.P. Mohamadi[1], A. Nemati[1], Z. Sadeghian*[2]

[1]Department of Materials Science and Engineering, Sharif University of Technology, Azadi street, P. O. Box 11155 – 4363 Tehran, Iran
[2]Research Institute of Petroleum Industry (RIPI), West Blvd. Azadi sport complex, P.O. Box 14857 – 3311, Tehran, Iran

received March 26, 2013; received in revised form June 12, 2013; accepted August 21, 2013

Abstract

This investigation focused on a comparison between hydroxyapatite (HA) and carbon-nanotube-reinforced hydroxyapatite composite (CNTs/HA) coatings. The HA and CNTs/HA composite (with 5 wt% CNTs) coatings were prepared with the sol-gel method on 316L stainless steel. Phase evaluation by means of XRD and Raman spectroscopy was performed on the HA and CNTs/HA composite coatings. The coatings were immersed in simulated body fluid (SBF) in order to evaluate the biological properties of the coatings. During the first week of immersion, the increase in the amount of Ca^{2+} precipitation in the SBF when CNTs/HA was used was lower than for the HA coatings. This behavior can be related to the difference in the amount of amorphous phases in the two types of coatings. The microstructure of the coatings was studied with AFM and SEM. The results showed that the crystallinity of the composite coating is greater than that of the HA coatings.

Keywords: hydroxyapatite, carbon nanotube, nanocomposite, bioactivity, in vitro test

I. Introduction

Hydroxyapatite ($(Ca_{10})(PO_4)_6(OH)_2$) is used for orthopedic and dentistry applications on account of its superior biological properties [1,2]. But its poor mechanical properties, such as low fracture toughness and brittleness, have limited its usage in high-load-bearing applications. To enhance the mechanical properties, other materials, such as zirconia [3], alumina [4] and CNTs [5–7], can be used as a second phase in the HA coating.

Carbon nanotubes have been an attractive choice as a reinforcing additive in polymers, metals and ceramics [8,9]. It has been shown that CNTs also have good bioactive potential [10], which is why there is interest in utilizing HA/CNTs composites to obtain better mechanical and biological properties for orthopedic applications [5,6].

The CNT-reinforced hydroxyapatite composite coating is a useful coating for high-load-bearing cases [11]. In another investigation conducted by Kealley *et al.* [12], hot isostatically pressed HA/CNTs samples exhibited excellent densification properties. In addition, phase analysis of the composites did not show any change in the structural parameters of the HA phase, with the exception of a slight reduction in the unit cell parameter [12]. Kaya [13] reported that the addition of carbon nanotubes increases the hardness, elastic modulus and interlaminar shear strength of monolithic hydroxyapatite layers. Balani *et al.* [14] addressed these issues based on the role of CNTs in improving fracture toughness (by 56 %) and enhancing crystallinity (by 27 %) of HA.

With regard to biological properties too, it has been shown that HA/CNTs composites can satisfy the requirements for biomaterials [15]. It is reported that CNTs have no cytotoxic effect when they are immobilized in a matrix [6]. Also HA/CNTs composite coatings have shown a significantly higher cell proliferation rate compared to pure HA coatings along with non-toxicity in the body environment [7,14]. In other research done by Bhattarai *et al.* [16], it has been reported that there is some evidence suggesting HA/CNTs composites could find application in nanotechnology for gene delivery systems.

In present study, *in vitro* characterization of HA/(5 wt%)CNTs composite coatings on 316L stainless steel obtained with the sol-gel method was conducted. The aim of the current work is to produce HA and HA/CNTs coatings and investigate their bioactivity based on immersion in SBF. The capacity of apatite precipitation from the SBF onto the immersed surface can be an indicator of its bioactivity [6,17].

II. Materials and Methods

HA and HA/CNTs composites were prepared by means of a sol-gel method developed in our previous work [9]. Phosphate and nitride solutions with a ratio of Ca/P = 1.67 were prepared and then the CNTs sol with the weight ratio of CNTs/HAP = 5. SDS was used as a surfactant to

* Corresponding author: Sadeghianz@ripi.ir

disperse the CNTs in water (weight ratio of SDS/CNTs was 4:1). 316L stainless steel substrates, with dimensions of 1 ×2 cm, were polished with 1200 sandpaper to obtain a rough surface as a substrate for the dip-coating procedure [18–20]. After being polished, the substrates were cleaned with acetone and distilled water and dip-coated. The dip-coating rate was 5 cm/sec. The coated specimens were heat-treated for 30 min at 350 °C [9]. The phase composition of both the composite and non-composite coatings was analyzed by means of X-ray diffraction. A Philips X'PERT MPD diffractometer with CuKα (1.5405 Å) radiation was devised for this purpose. Raman spectroscopy was also performed on both coatings with an Almega Raman spectrometer with a wavelength of 514.5 nm in Ar atmosphere at room temperature. The heat-treated coatings were immersed in the SBF solution for different periods between one and four weeks. The purpose of immersion in SBF was precipitation of HA on the coatings to study the bioactivity of the implants. The solution was prepared according to Kokubo's procedure [21]. The resulting solution has almost the same composition as human blood plasma. During the immersion period, the concentration of Ca^{2+} was measured with ICP (Shimadzu, model ICPS–700, ver. 2) analysis. The Ca^{2+} concentration was measured once every three days and after each term the SBF was replaced with new SBF solution. After immersion, microstructure, surface roughness and morphology of the coatings were studied with AFM (NanowizardII, Germany) and SEM (XL-30 Philips, Holland).

III. Results and Discussion

(1) XRD analysis

XRD analysis was conducted on both the HA and HA/CNTs coatings. The analysis results showed that the heat-treated coatings have a crystalline structure (Fig. 1). They showed that the degree of crystallization of the HA/CNTs is greater than that of the HA, which may be attributed to the positive effect of CNTs on the crystallization of HA as reported in earlier studies [14]. The XRD pattern indicated only peaks corresponding to pure stoichiometric HA (JCPDS Card No. 9–432) in both coatings and peaks of CNTs (JCPDS card No. 41–1487) only in the HA/CNTs coating. Both patterns showed an amorphous background, which is because of the low heat treatment temperature (350 °C).

(2) Raman spectroscopy

The composite coating was also characterized with Raman spectroscopy in order to verify the presence of CNTs. The Raman spectroscopy was performed in the range of 1000–2000 cm^{-1} with a laser wavelength of 785 nm. The tangential (G band) and disordered mode (D band) of carbon atoms in the spectra (Fig. 2) indicate that there has been no significant chemical reaction between the HA and CNTs during the preparation of the coatings [22].

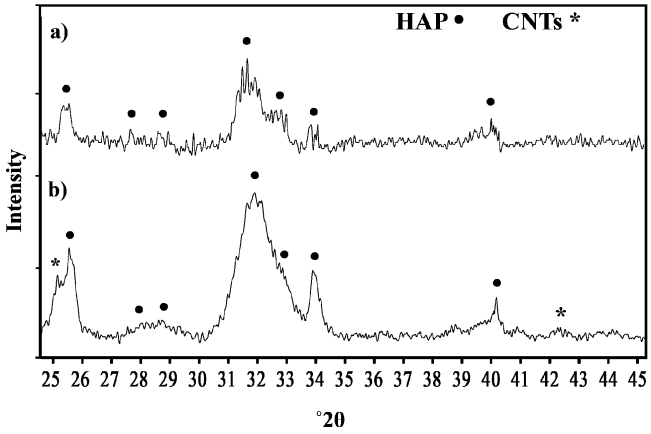

Fig. 1: XRD pattern of a) HA and b) HA/CNTs composite coatings.

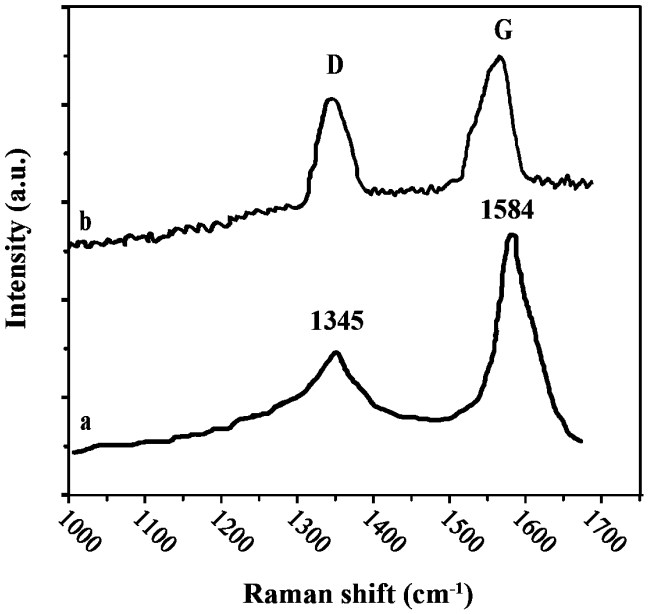

Fig. 2 : Raman spectra of a) CNTs [23] and HA/CNTs composite coating.

(3) ICP analysis

The concentration of Ca^{2+} in the SBF solution was measured in 3-day periods. The results are shown in Fig. 3. In the first three days of immersion, the Ca^{2+} concentration in the SBF increased. Different studies have indicated that the CNTs surface is suitable for apatite precipitation from SBF. For the CNTs/HA composites, it has also been revealed that CNTs have a positive effect on apatite formation [6].

The second measurement again showed Ca^{2+} super-saturation. But the concentration decreased compared to the first measurement. These results are in good agreement with the theory that super-saturation of Ca^{2+} ions in SBF along with the porous surface structure accelerate the nucleation of apatite phase [17, 24]. The increase in the Ca^{2+} concentration in the HA coating was higher than that in the HA/CNTs coating. It seems that is because of the different amount of amorphous phases that are more disposed to dissolution in SBF. A more amorphous background in the pure HA coating was detected by means of XRD.

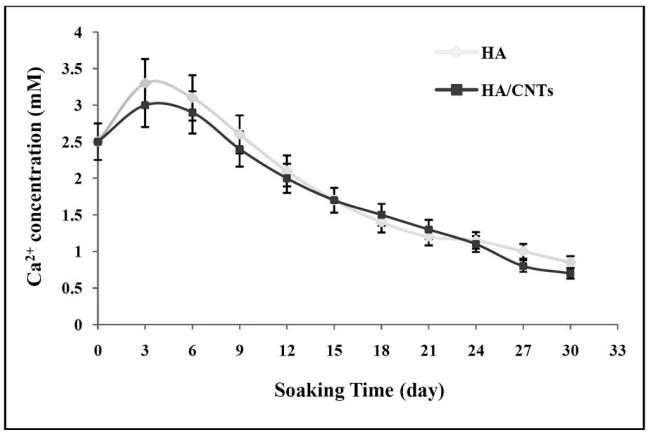

Fig. 3: Ca^{2+} concentration of HA and HA/CNTs composite in SBF versus immersion time.

Release of ions into SBF increases the activity of the ions that comprise the bone-like apatite and causes nucleation and growth of apatite on the surface. With the release of calcium and phosphate ions, the surface of HA will be negatively charged. This surface attracts the calcium ions and is a suitable homogenous nucleation site for apatite [25, 26]. It is well known that precipitation of HA from SBF on a bioactive surface occurs as part of a complex process. With the increase in the supersaturation of Ca^{2+} in the coating-SBF interface, precipitation of metastable calcium phosphate phases starts. These phases simultaneously dissolve in the SBF. In this way, the metastable phases act as a precursor during the precipitation process. When calcium-phosphate ceramics are soaked in SBF, the precursor phase is octa-calcium phosphate (OCB), which serves as a template for HA formation on the bioactive surface [27]. During the last days of immersion, the concentration of Ca^{2+} decreases, which is evidence of HA precipitation on the surface of the coatings.

CaO, TCP and TTCP may also dissolve in SBF. CaO, TCP and TTCP phases were not detected in the XRD pattern and we have no other evidence of their existence in the coating [25]. It is believed that the CNTs surface is a preferable position for apatite mineralization. This fact along with greater crystallinity of the composite itself is a noticeable advantage of a stable scaffold structure [14].

(4) AFM and SEM images

Figs. 4 and 5 show the roughness and morphology of surfaces after immersion in SBF at different times. The surface roughness increased during the first week of immersion in the SBF but after seven days of immersion a smooth surface was observed. In this microstructure more distinct grains can be recognized. Surface roughness decreased during the second week and after that period the roughness of surfaces started to increase again. Changes of roughness are in a good agreement with results obtained earlier in which the changes in the Ca^{2+} concentration in SBF were studied showing that during the immersion of coatings in SBF, Ca^{2+} concentration increased in the earlier days of immersion and after that started to decrease. It means some phases started to dissolve in the SBF immediately after immersion and after that, HA started to deposit on the surface [27, 29, 30]. It seems the increase in roughness during the first week of soaking in the SBF is because of the dissolution of some calcium phosphate phases. Deposition of HA from the SBF onto the surface of the coating caused the surface roughness to increase after six days of immersion. It is suggested that surface pores and microcracks are preferable positions for primary apatite nucleation, because these situations are in the immediate vicinity of the super-saturated environment [17]. Growing the new apatite layer, seeded from the pores of the rough surface, makes the surface smoother up to the second week. But more growth of the apatite layer after that time increases the surface roughness.

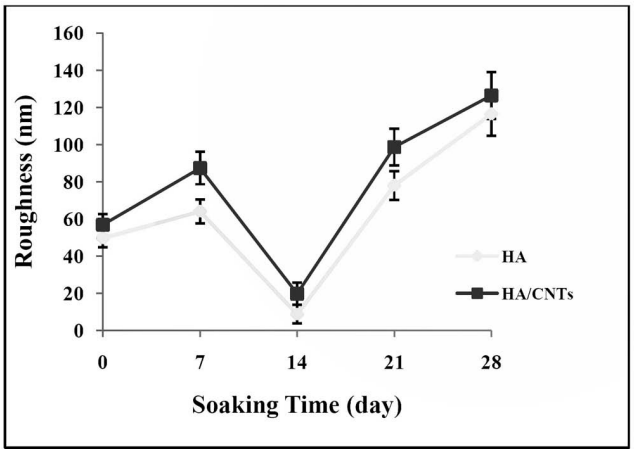

Fig. 4: Surface roughness of specimens before and after immersion in SBF.

After 14 days of immersion, surfaces completely covered with spherical grains were detected on both the HA and CNTs/HA coatings. This surface has been composed after precipitation of a new apatite layer on the coatings. The structure of this apatite layer composed on the HA/CNT coating contains smaller grains than that of the pure HA coating. This phenomenon shows the positive effect of CNTs in the composite coating on nucleation of new apatite grains from SBF. This conclusion is also supported by the XRD results, which showed a more crystalline structure in the composite coatings. At later times, the only observation is formation of coarse apatite layer on the surfaces. There is no significant difference between the AFM microstructure of the composite and non-composite coatings in these periods of immersion (after 21 and 28 days).

Microstructural changes of HA and HA/CNTs composite coatings were also monitored with SEM (Fig. 6). Arrows in the HA/CNTs composite coating indicate CNTs distributed throughout the coating. It is obvious that the composite coating has a coarser and more porous surface. Although a distinct granular structure does not appear in non-heat-treated coatings, the composite coating appears to have more crystalline structure with finer particles (Fig. 6a). After the first week of immersion, the microstructure of coatings became gradually coarser with wide pores. This structure has been created as a result of the dissolution of some phases from the surface into the SBF (Fig. 6b). After the second week of soaking,

a smoother surface is formed in both the composite and non-composite coatings (Fig. 6c). As mentioned earlier, this structure resulted from nucleation and growth of apatite phase into the pores of coatings. These positions that are surrounded with super-saturated SBF are suggested as preferable nucleation sites. The apatite layer continued to grow until it became a thicker and denser layer afterthird andfourth weeks of immersion (Figs. 6d, 6e). The apatite layer observed on days 14 and 21 formed on composite coating is more porous compared with the pure HA. Also after 14 days of immersion, a more granular structure of precipitated HA appears on the composite surface. It indicates that there may be more bioactive potential in the composite coating for bone tissue ingrowth.

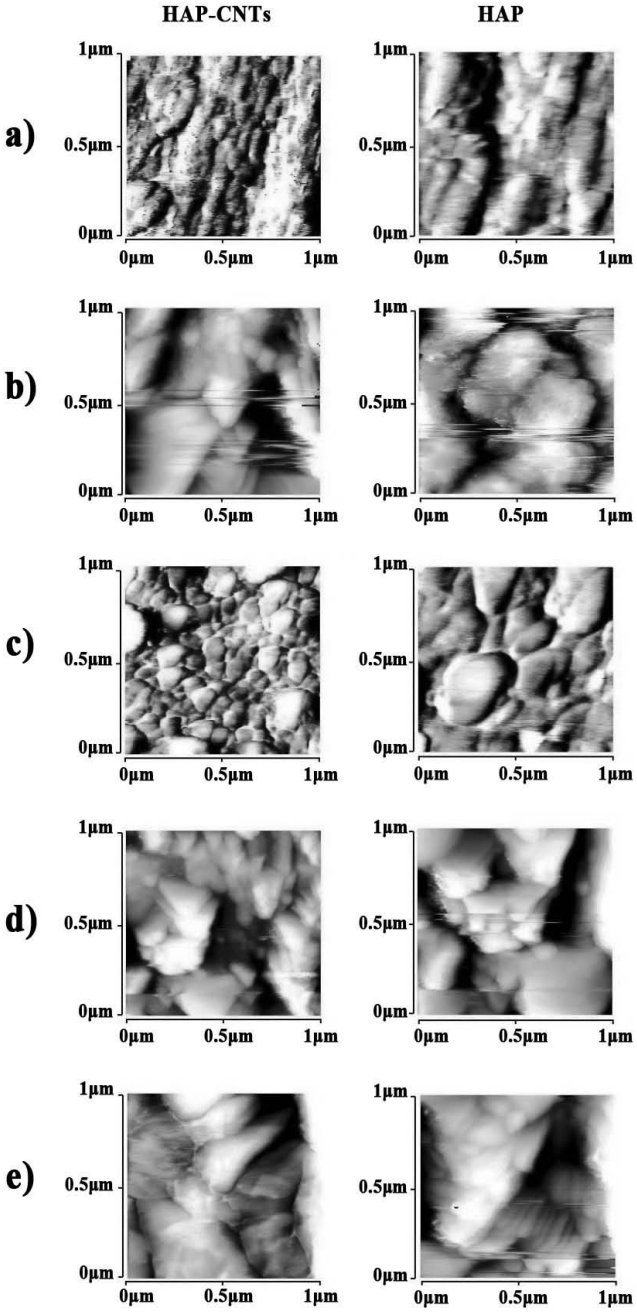

Fig. 5: AFM images of HA and HA/CNTs coatings before and after immersion in SBF (for 1, 2, 3, 4 weeks).

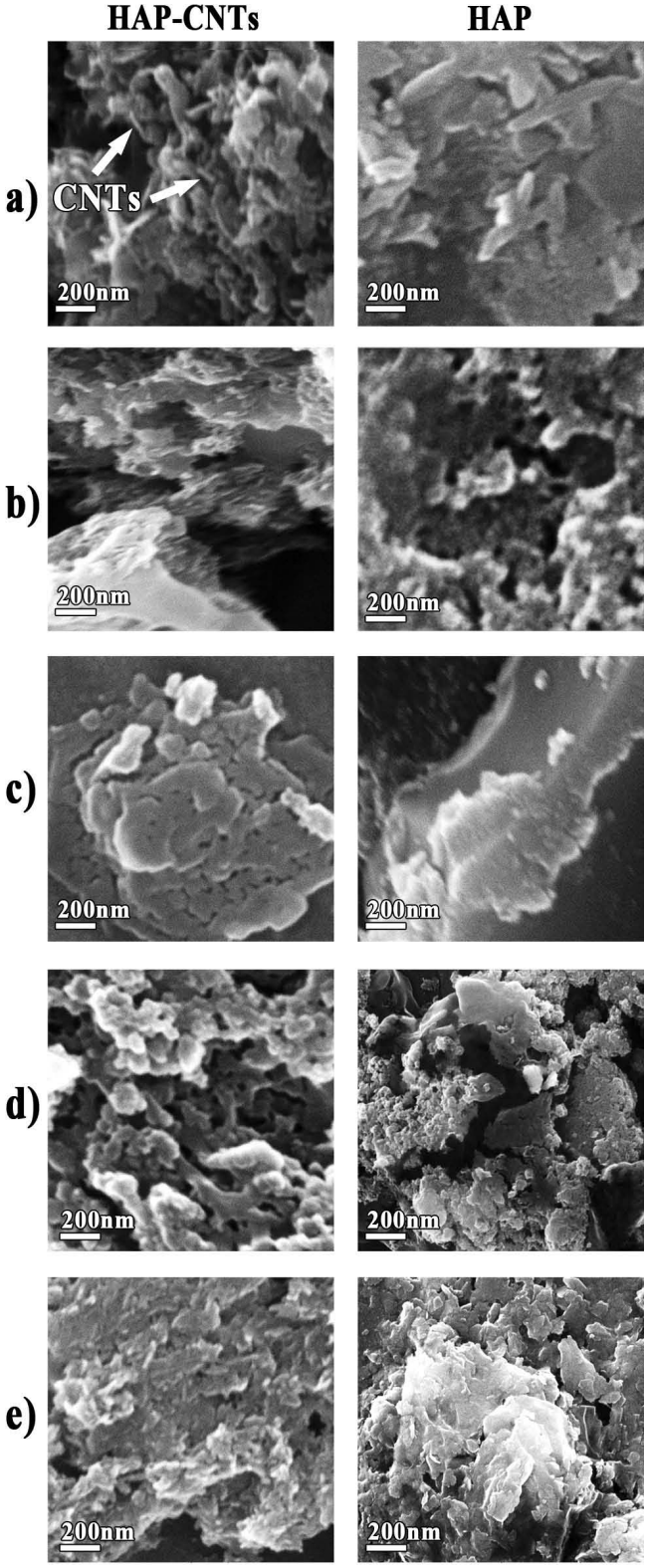

Fig. 6 : SEM images of HA/CNTs coatings (a) before and (b, c, d, e) after immersion in SBF (for 1, 2, 3, 4 weeks).

IV. Conclusions

Phase evaluation performed by means of XRD analysis presented evidence of the positive effect of CNTs in the crystallization of HA. Raman spectroscopy also showed the presence of CNTs in the composite structure without noticeable decomposition. ICP results indicated an active response of HA and HA/CNTs coatings in the SBF, that was the dissolution of HA into the solution in first

week and then deposition of HA from the solution in the following weeks. SEM surface morphologies also suggest that CNTs increase the HA nucleation sites, which is also supported by the ICP results. Surface roughness evaluated with AFM and SEM microscopy images were subsidiary evidence of the ICP results and bioactive behavior of coatings.

References

1 Hench, L.L.: Bioceramics: from concept to clinic, *J. Am. Ceram. Soc.*, **74**, 487 – 510, (1991).

2 Jarcho, M.: Calcium phosphate ceramics as hard tissue prosthetics, *Clin. Orthop. Relat. R.*, **157**, 59 – 78, (1981).

3 Gu, Y.W., Khor, K.A., Pan, D., Cheang, P.: Activity of plasma sprayed yttria stabilized zirconia reinforced hydroxyapatite/Ti-6Al-4V composite coatings in simulated body fluid, *Biomaterials*, **25**, 77 – 85, (2004).

4 Evis, Z., Doremus, R.H.: Coatings of hydroxyapatite-nanosize alpha alumina composites on Ti-6Al-4V, *Mater. Lett.*, **59**, 3824 – 7, (2005).

5 White, A.A., Best, S.M., Kinloch, I.A.: Hydroxyapatite-carbon nanotube composites for biomedical applications: a review, *Int. J. Appl. Ceram. Tech.*, **4**, (1), 1 – 13, (2007).

6 Lahiri, D., Ghosh, S., Agarwal, A.: Carbon nanotube reinforced hydroxyapatite composite for orthopedic application: A review, *Mat. Sci. Eng. C*, **32**, 1727 – 1758, (2012).

7 Hahn B.D., Lee, J.M., Park, D.S.: Mechanical and *in vitro* biological performances of hydroxyapatite-carbon nanotube composite coatings deposited on Ti by aerosol deposition, *Acta Biomater.*, **5**, 3205 – 3214, (2009).

8 Jackson, J., Ahmed, W.: Applications of Carbon Nanotubes in Bio-Nanotechnology, in Surface Engineered Surgical Tools and Medical Devices, Eds. Springer Science+Business Media LLC, New York, NY, USA, pp. 439 – 475, 2007.

9 Najafi, H., Nemati, A., Sadeghian, Z.: Inclusion of carbon nanotubes in a hydroxyapatite sol-gel matrix, *Ceram. Int*., **35**, 2987 – 2991, (2009).

10 Spanos, N., Misirlis, D.Y., Kanellopoulou, D.G., Koutsoukos. P.G.: Seeded growth of hydroxyapatite in simulated body fluid, *J. Mater. Sci.*, **41**, 1805 – 1812, (2006).

11 Chen, Y., Zhang, Y.Q., Zhang, T.H., Gan, C.H., Zheng, C.Y., Yu, G.: Carbon nanotube reinforced hydroxyapatite composite coatings produced through laser surface alloying, *Carbon*, **44**, 37 – 45, (2006).

12 Kealley, C., Elcombe, M., Riessen, A.V., Ben-Nissan., B.: Development of carbon nanotube-reinforced hydroxyapatite bioceramics, *Physica B*, **385 – 386**, 496 – 498, (2006).

13 Kaya, C.: Electrophoretic deposition of carbon nanotube-reinforced hydroxyapatite bioactive layers on Ti-6Al-4V alloys for biomedical applications, *Ceram. Int.*, **34**, 1843 – 1847, (2007).

14 Balani, K., Anderson, R., Laha, T., Andara. M.: Plasma-sprayed carbon nanotube reinforced hydroxyapatite coatings and their interaction with human osteoblasts in vitro, *Biomaterials*, **28**, 618 – 624, (2007).

15 Li, A., Sun, K., Dong, W., Zhao, D.: Mechanical properties, microstructure and histocompatibility of MWCNTs/HAp biocomposites, *Mater. Lett.*, **61**, 1839 – 1844, (2007).

16 Bhattarai, S.R., Aryal, S.: Carbon nanotube-hydroxyapatite nanocomposite for DNA complexation, *Mat. Sci. Eng. C*, **28**, 64 – 69 (2008).

17 Weng, J., Liu, Q., Wolke, J.G.C., Zhang, X., de Groot, K.: Forming and characteristics of the apatite layer on plasma sprayed hydroxyapatite-coatings in simulated body fluid, *Biomaterials*, **18**, 1027 – 1035, (1997).

18 Park, J.-H., Lee, D.Y., Oh, K.T., Lee, Y.K.: Bioactivity of calcium phosphate coatings prepared by electrodeposition in a modified simulated body fluid, *Mater. Lett.*, **60**, 2573 – 2577, (2006).

19 Zhang, Q., Leng, Y., Xin, R., Wang, C., Lu, X., Chen, J.: An effective approach to activate 316L stainless steel for biomimetic coating of calcium phosphate, *J. Mater. Sci.*, **42**, 6205 – 6211, (2007).

20 Wang, Y., Sam, Z., Zeng, X., Cheng, K., Qian, M., Weng, W.: *In vitro* behavior of fluoridated hydroxyapatite coatings in organic-containing simulated body fluid, *Mater. Sci. Eng. C*, **27**, 244 – 250, (2007).

21 Kokubo, T., Takadama. H.: How useful is SBF in predicting *in vivo* bone bioactivity?, *Biomaterials*, **27**, 2907 – 2915, (2006).

22 Xu, J.L., Khor, K.A., Sui, J.J., Chen, W.N.: Preparation and characterization of a novel hydroxyapatite/carbon nanotubes composite and its interaction with osteoblast-like cells, *Mater. Sci. Eng. C*, **29**, 44 – 49, (2009).

23 Sadeghian, Z.: Large scale production of multi-walled carbon nanotubes by low-cast spray pyrolysis of hexane, *New Carbon Mater.*, **24**, 33 – 37, (2009).

24 Guo, Y., Yao, Y.B., Ning, C.Q., Chu, L.F., Guo, Y.J.: Fabrication of mesoporous carbonated hydroxyapatite/carbon nanotube composite coatings by microwave irradiation method, *Mater. Lett.*, **65**, 1007 – 1009, (2011).

25 Li, P., Yang, Q., Zhang, F., Kokubo, T.: The effect of residual glassy phase in a bioactive glass-ceramic on the formation of its surface apatite layer *in vitro*, *J. Mater. Sci: Mater. M.*, **3**, 452 – 456, (1992).

26 Rath, P.C., Singh, B.P., Besra, L., Bhattacharjee S.: Multi-walled carbon nanotubes reinforced hydroxyapatite-chitosan composite coating on Ti metal: Corrosion and mechanical properties, *J. Am. Ceram. Soc.*, **95**, [9], 2725 – 2731, (2012).

27 Kweh, S.W.K., Khor, K.A., Cheang, P.: An *in vitro* investigation of plasma sprayed hydroxyapatite (HA) coatings produced with flame-spheroidized feedstock, *Biomaterials*, **23**, 775 – 785, (2002).

28 Grassmann, O., Heimann, R.B.: Compositional and microstructural changes of engineered plasma sprayed hydroxyapatite coatings on Ti-6Al-4V substrates during incubation in protein-free simulated body fluid, *J. Biomed Mater. Res.*, **53**, 685 – 693, (2000).

29 Luo, Z.S., Cui, F.Z., Feng, Q.L., Li, H.D., Zhu, X.D., Spector, M.: *In vitro* and *in vivo* evaluation of degradability of hydroxyapatite coatings synthesized by ion beam-assisted deposition, *Surf. Coat. Tech.*, **131**, 192 – 195, (2000).

30 Wang, Y., Zhang, S., Cheng, K., Qian, M., Weng, W.: *In vitro* behavior of fluoridated hydroxyapatite coatings in organic-containing simulated body fluid, *Mater. Sci. Eng. C*, **27**, 244 – 250, (2007).